



ARTICLE

Enhancing the Properties of Biodegradable Food Packaging Films Derived from Agar and Porang-Glucomannan (*Amorphophallus oncophyllus*) Blends

Toni Dwi Novianto^{1,2}, Sri Rahayoe^{1,*} and Bakti Berlyanto Sedayu^{2,*}

¹Department Agricultural and Biosystem Engineering, Faculty of Agricultural Technology, Gadjah Mada University, Yogyakarta, 55281, Indonesia

²Research Center for Food Technology and Processing, National Research and Innovation Agency of the Republic of Indonesia, Yogyakarta, 55861, Indonesia

*Corresponding Authors: Sri Rahayoe. Email: srahayoe@ugm.ac.id; Bakti Berlyanto Sedayu. Email: bakt002@brin.go.id

Received: 14 August 2024 Accepted: 14 September 2024 Published: 20 February 2025

ABSTRACT

This study aimed to develop and characterize biodegradable packaging film from blends of two natural polysaccharides, i.e., agar and glucomannan. The glucomannan used was derived from the specific tuber plant *Amorphophallus oncophyllus* (locally known as “porang”), which grows abundantly in Indonesian forests and remains underutilized. Various ratios of agar and porang-glucomannan (PG) proportions were formulated to produce a food packaging film, which was subsequently tested for its mechanical, physical, chemical, and thermal properties. The results showed that the inclusion of PG to the film formulations notably enhanced the stretchability of agar films, achieving maximum a twofold increase, while concurrently reducing their water resistance such as increased water solubility and water swelling for up to 125% and 105%, respectively. The mechanical and thermal properties, as well as the water vapor permeability of the resulting film, were significantly affected by the polymer matrix structure formed by the varying proportions of the two biopolymers. The enhancement of these properties was associated with a more solid/compact film structure, as corroborated by cross-sectional images obtained through SEM analysis. The study’s findings suggest that utilizing agar and porang biomass has significant potential for further development as an environmentally friendly food packaging material.

KEYWORDS

Agar; *Amorphophallus oncophyllus*; biodegradable; film; glucomannan; porang

Nomenclature

PG	Porang glucomannan
TS	Tensile strength
EAB	Elongation at break
TGA	Thermogravimetric analysis
dTG	Derivative thermogravimetric
T_g	Glass transition temperature
T_m	Melting temperature
DSC	Differential scanning calorimetry



1 Introduction

Ensuring the safety and quality of food considerably depends on effective packaging materials, and to date, fossil fuel-based synthetic packaging is still commonly used. This material has benefited the food industries due to its affordability, inherent lightweight, and strong barrier properties [1]. However, its disposal leads to greenhouse gas emissions and environmental damage. Plastic waste accumulation in landfills and oceans also exacerbates these problems, causing pollution and harm to wildlife [2]. Hence, there has been a surge in innovation and research into biodegradable materials or bioplastics that can maintain food safety and quality while minimizing environmental impact [3,4].

Seaweed has been identified as a promising biomass for bioplastic raw material, especially in an archipelagic nation such as Indonesia [5]. With its long coastlines, the region provides ideal conditions for seaweed farming, particularly species of red algae (*Rhodophyceae*) such as *Gracilaria* sp., which is renowned for its agar production [5]. Previous studies have demonstrated that agar-based films offer great barrier properties against water vapor compared to other biopolymer-based films [6,7]. However, agar-based films tend to be brittle and have poor stretchability due to their inherent properties [8], which consequently limits their practical applications such as for packaging film. Therefore, their mechanical properties need to be enhanced. One effective approach is through blending agar with other biopolymers, such as glucomannan [9,10].

Glucomannan is a natural polysaccharide extracted from tuber plants of the genus *Amorphophallus*, which includes approximately 170 species worldwide [11]. The glucomannan extracted from different species typically varies in its physicochemical properties, such as chemical composition, water holding capacity (WHC), and viscosity [12]. Among these species, *Amorphophallus oncophyllus*, commonly known as ‘porang,’ is particularly abundant in Indonesian forests and is a rich source of glucomannan, with concentrations typically ranging from 50%–65% [13]. However, the consumption of porang is generally unfavorable due to high levels of calcium oxalate, which can cause itching and other health issues [14].

The glucomannan extracted from “porang” (referred to in this paper as porang-glucomannan or PG) is promising for bioplastic film materials due to its higher solubility, acetylation degree, lower WHC, viscosity, and degree of polymerization compared to commercially available glucomannan [15]. Based on an in-depth literature review conducted by the authors, it was found that there is still very limited research that explores the utilization of glucomannan for the production of environmentally friendly bioplastic films, particularly that which is derived from the tuber species *Amorphophallus oncophyllus*. A few recent studies on the use of porang as a packaging film have focused on incorporating plasticizers and active ingredients to develop edible films [16,17]. Additionally, the authors did not find any studies that investigate the blending of agar and PG polymers, highlighting a significant gap in the existing research in bioplastic field. By blending agar with PG, the resulting bioplastic films were expected to exhibit improved mechanical strength, particularly the flexibility, also other performance. Several previous studies have also reported that incorporating glucomannan extracted from species *Amorphophallus konjac* can enhance the mechanical properties of edible films made from gelatin and *Aloe vera* [14,18].

Hence, this study investigated how different proportions of agar and glucomannan affect the mechanical strength, physicochemical, and barrier properties, as well as the thermal stability of the agar-porang glucomannan bioplastic films. The goal was to develop a biodegradable film with enhanced properties suitable for food packaging. This approach also aimed to achieve the desired film characteristics in a cost-effective manner while simultaneously enhancing the value of local commodities.

2 Materials and Methods

2.1 Materials

The materials used for film preparation included commercial agar powder supplied by CV. Sari Mutiara Abadi (Malang, Indonesia). The agar has specifications of a 4296 kDa molecular weight, 9% moisture content, 0.89% sulfate content, and 793 g/cm² gel strength. Porang-glucomannan flour (PG) was supplied by the Faculty of Agricultural Technology at Gadjah Mada University with a glucomannan content of 97.57%, viscosity of 40,000 m.pas, and whiteness value of 82% [19], pharmaceutical grade glycerol with a molecule weight (Mw) of 92.093 g/mol from Rofa Laboratorium Centre (Bandung, Indonesia), and distilled water were used as the plasticizer and casting solution, respectively.

2.2 Bioplastic Film Preparation

The films were prepared through solvent casting following the procedure outlined by Qiao et al. [9] with slight modifications. The films consisted of a mixture of agar and PG with varying ratios of 100:0, 75:25, 50:50, 25:75, and 0:100 (w/w), which were respectively labeled as **A₁₀₀P₀**, **A₇₅P₂₅**, **A₅₀P₅₀**, **A₂₅P₇₅**, and **A₀P₁₀₀**. A total of 2 grams of agar/PG was dissolved in 150 mL of distilled water, ensuring thorough mixing by a hotplate with a stirrer for 10 min. Subsequently, 1 gram of glycerol was added, and the stirring temperature was increased to 90°C, with stirring continued for an additional 30 min. Subsequently, 60 mL of the solution was poured into a rectangular stainless tray measuring 6 × 17 cm² and allowed to dry in an oven at 50°C for 24 h. Once dried, the films were taken out from the tray and placed in a desiccator containing a saturated Mg(NO₃)₂ solution to maintain a relative humidity of 52% for 48 h before undergoing characterization tests.

2.3 Film Characterization

2.3.1 Thickness

The thickness of each sample was assessed using a digital thickness gauge with a precision of 0.01 mm at ten randomly selected points [20].

2.3.2 Water Sensitivity

The measurement of the weight loss percentage of the sample film after drying was done to determine the moisture content, following the method described by Valizadeh et al. [21]. Film specimens measuring 1.5 × 1.5 cm² were dried for 24 h in an oven set at 105°C. The weight before and after drying was recorded to calculate the moisture content of each sample.

The water solubility and swelling were determined following the method of Xiao et al. [22] with minor modifications. Initially, film samples measuring 1.5 × 1.5 cm² were dried in an oven at 105°C for 24 h (*m*₀). Subsequently, the samples were immersed in 30 mL of distilled water for 24 h. The film samples were then carefully removed and re-dried in an oven at 105°C for 24 h. The sample weights were measured (*m*₁), and water solubility was calculated using the following Eq. (1):

$$\% \text{ Solubility} = \frac{m_0 - m_1}{m_0} \times 100\% \quad (1)$$

where *m*₀ is the initial dry weight of the sample, and *m*₁ is the weight of the dried sample after 24 h of immersion.

The water swelling was measured by drying a 1.5 × 1.5 cm² sample in an oven at 105°C for 24 h (*m*₀). Afterward, it was immersed in 30 mL of deionized water for 3 h. Subsequently, the film samples were carefully taken out, and their surfaces were gently wiped with absorbent before being re-weighed (*m*₁). The calculation of water swelling followed the equation below (2):

$$\% \text{ Swelling} = \frac{m1 - m0}{m0} \times 100 \% \quad (2)$$

where $m0$ is the initial dry weight of the sample, and $m1$ is the weight of the sample after 3 h of immersion.

2.3.3 Opacity

The film's opacity was assessed using a UV-Vis spectrometer (Cary 5000, Agilent, Santa Clara, CA, US) at a wavelength of 550 nm. Film strips sized $0.8 \times 5 \text{ cm}^2$ were placed into a cuvette. An empty cuvette was used as the calibration standard. The opacity was calculated using the following Eq. (3):

$$\text{Opacity} = \frac{\text{Abs}/550}{x(\text{mm})} \quad (3)$$

whereas the *Abs* represents the absorbance at wavelengths of 550 nm, and x represents the thickness of the film in millimeters.

2.3.4 Mechanical Strength

The tensile strength (TS) and elongation at break (EAB) of the film were assessed using a Shimadzu AGS-X series 10 kN Universal Testing Machine (UTM), following the ASTM D882 standards. Film strips sized $6 \times 1.5 \text{ cm}^2$ were subjected to a 5 kN load at a rate of 10 mm/min following the procedure done by Sedayu et al. [23].

2.3.5 FTIR (Fourier-Transform Infrared)

The chemical structure differences among the sample films were observed using an FTIR Spectrometer Vertex 80 (Bruker, Germany) equipped with attenuated total reflection (ATR). The samples sized at $1.5 \times 1.5 \text{ cm}$ were prepared for analysis within a wavelength range of $600\text{--}4000 \text{ cm}^{-1}$ [24].

2.3.6 Thermal Properties

A differential scanning calorimetry (DSC) analysis was performed using a DSC 60 instrument by Shimadzu (Kyoto, Japan). For this testing, a 4 mg sample was mounted in a 40 μL aluminum pan and gradually heated from 30°C to 400°C under a nitrogen atmosphere, with a heating rate of 10°C per minute. In addition, a thermogravimetric analysis (TGA) was carried out using a Simultaneous Thermal Analyzer STA 6000 from Perkin Elmer. A 10–15 mg of sample was loaded into crucible pans and subjected to a gradual temperature increase from 30°C to 500°C at a rate of 10°C per minute. The heating process was under a flowing nitrogen gas atmosphere [25].

2.3.7 Water Vapor Permeability (WVP)

Water vapor permeability (WVP) was determined in accordance with a method outlined by Sedayu et al. [23]. Circular samples with a diameter of 0.8 mm were clamped between the lips of vials sealed with caps. Silica gel was placed inside the vials to achieve an internal relative humidity (RH) of 0%. The prepared vials were then placed on a rack and stored in a desiccator filled with water underneath, creating an environment with saturated water vapor (100% RH). Subsequently, the desiccator was kept in an incubator to maintain a stable temperature. The weight of each vial was measured daily for six days, and WVP was calculated using the following Eq. (4):

$$\text{WVP} = \frac{x}{\Delta P} \times \frac{w}{tA} \quad (4)$$

with x represents the film thickness (mm), ΔP is the difference in partial pressure (Pa) of water passing through the film, w is the weight of the vial (g) at the time t (days), and A is the film's surface area (cm^2).

2.3.8 Scanning Electron Microscopy

The cross-sectional images of the film were observed using a Hitachi SU3500 scanning electron microscope (SEM). Before being subjected to the machine, the samples were pre-coated with gold for 60 s under vacuum conditions. The instrument operated at a voltage acceleration of 3 kV in a vacuum condition, and the samples were visualized at 1000× magnification.

2.4 Statistical Analysis

The experimental data were collected and processed statistically using one-way analysis of variance (ANOVA). Subsequently, the Tukey test was applied for further analysis to identify significant differences among the various film formulations, with a confidence interval value of $p < 0.05$.

3 Result and Discussion

3.1 Thickness and Water Sensitivity

The thickness of a bioplastic film is among the most substantial parameters since it could affect other characteristics such as transparency, mechanical strength, or barrier properties. The measurements showed a relatively uniform thickness of the film samples across all formulations, which are ranging from 0.07 to 0.08 mm (Table 1). The thickness of the agar films was not significantly changed after the blending with PG ($p > 0.05$). This may be due to the similarity in physical properties, such as density or the dimensional polymer matrix structure, between those two polymers. As a result, variations in their proportions in the film formation did not result in differences in thickness.

Table 1: Physical properties and water sensitivity of agar/PG bioplastic films: A₁₀₀P₀ = 100:0, A₇₅P₂₅ = 75:25, A₅₀P₅₀ = 50:50, A₂₅P₇₅ = 25:75, and A₀P₁₀₀ = 0:100 of the agar and PG ratios (% w/w)

Film samples	Thickness (mm)	Moisture content (%)	Water solubility (%)	Water swelling (%)
A ₁₀₀ P ₀	0.08 ± 0.00 ^a	16.37 ± 0.24 ^a	16.51 ± 0.63 ^a	97.38 ± 074 ^a
A ₇₅ P ₂₅	0.08 ± 0.01 ^a	17.45 ± 0.06 ^{ab}	21.63 ± 0.28 ^b	125.41 ± 2.96 ^b
A ₅₀ P ₅₀	0.07 ± 0.01 ^a	19.05 ± 0.03 ^b	24.26 ± 0.19 ^c	200.11 ± 5.04 ^d
A ₂₅ P ₇₅	0.08 ± 0.01 ^a	19.58 ± 0.14 ^b	37.11 ± 0.29 ^d	180.02 ± 1.89 ^c
A ₀ P ₁₀₀	0.08 ± 0.01 ^a	19.48 ± 1.94 ^b	100 ± 0.00 ^e	NA

Note: Values are given as mean ± standard deviation. Different letters within the same column indicated significant differences ($p < 0.05$).

The moisture content of agar/PG films ranged from 14.08% to 19.58% (wb). The results notably indicate that the inclusion of PG significantly affects the moisture content of the produced films ($p < 0.05$) with higher amounts of PG in the matrix leading to increased moisture content (see Table 1). Agar and PG are both hydrophilic polysaccharides since their chemical structures contain numerous hydroxyl groups [26,27]. This hydrophilicity allows them to interact with and bind water molecules. However, the sample films predominated by PG exhibit higher moisture content due to the inherent polymeric structure of this polysaccharide. Unlike agar, PG may have more flexible and open polymer chains, which allow greater water absorption and retention [28]. Such a chemical structure of PG enables its polymeric film to bind more water molecules than agar. In addition, the increased hydrophilicity due to PG incorporation was followed by higher water sensitivity of the produced films. In other words, the increased proportion of PG in the polymer matrix reduces the water resistance of the films. This is evident by its greater solubility in water and its significant swelling when in contact with water, showing a similar trend

observed in the moisture content results. The test results indicated that both water solubility and water swelling of the pure agar films increased, reaching 125% and 105%, respectively, when 75% PG (A₂₅P₇₅) and 50% PG (A₅₀P₅₀) were added to the film formulation. It is also worth noting that the films made from 100% pure PG were completely dissolved after immersion in water for 24 h, resulting in the swelling data being unidentifiable (see Table 1).

For food packaging applications, the water resistance of packaging film stands out as a critical parameter. For example, in the context of edible packaging purposes, a low or moderate water solubility may be preferable in particularly for ready-to-eat products. However, for high-moisture foods such as fruits and meat, a high-water-resistance material is more desirable to maintain the integrity of the packaging and prevent it from easily deteriorating [29,30]. Additionally, moisture content is also a crucial parameter for bioplastic film quality, as it influences both barrier and mechanical properties [31].

3.2 Optical, Tensile, and Barrier Properties

As presented in the Table 2, the opacity of the sample films increased with a higher amount of PG in the film formulation. This phenomenon may be attributed to the presence of impurities originating from PG, such as compounds like starch, protein, and ash, which obstruct light transmission through the film membrane [13]. In addition to this, the less clean appearance (brownish color) of PG may also result from the refining and grinding processes during the PG production [32]. This property is important for showcasing the visibility of packaged food and influencing consumer acceptance levels [33].

Table 2: Optical, and tensile properties of agar/PG bioplastic films: A₁₀₀P₀ = 100:0, A₇₅P₂₅ = 75:25, A₅₀P₅₀ = 50:50, A₂₅P₇₅ = 25:75, and A₀P₁₀₀ = 0:100 of the agar and PG ratios (% w/w)

Film samples	Opacity	Tensile strength (N/mm ²)	Elongation at break (%)
A ₁₀₀ P ₀	3.78 ± 0.02 ^a	60.91 ± 5.79 ^b	11.03 ± 2.34 ^a
A ₇₅ P ₂₅	4.64 ± 0.07 ^c	83.71 ± 3.62 ^c	22.24 ± 6.04 ^{ab}
A ₅₀ P ₅₀	4.59 ± 0.1 ^c	78.87 ± 3.69 ^c	15.79 ± 6.79 ^{ab}
A ₂₅ P ₇₅	4.31 ± 0.03 ^b	67.40 ± 2.29 ^b	20.48 ± 6.38 ^{ab}
A ₀ P ₁₀₀	5.55 ± 0.1 ^d	45.58 ± 0.66 ^a	27.11 ± 6.48 ^a

Note: Values are given as mean ± standard deviation. Different letters within the same column indicated significant differences ($p < 0.05$).

Table 2 shows that adding the proportion of PG up to 25% in the film's formulation (A₇₅P₂₅) significantly increases the tensile strength (TS) of the agar film ($p < 0.05$) resulting in a 38% increase. However, when the PG content exceeds this proportion, the TS begins to decrease reaching its lowest value of 45.58 MPa for the pure PG film (A₀P₁₀₀). Moreover, the elongation at break (EAB) values generally increase as the proportion of PG in the film matrix rises with the maximum increase observed at 25% PG (A₇₅P₂₅), resulting in more than a twofold increase.

The interaction between agar and porang-glucomannan at certain composition ratios within the polymer matrix results in the formation of a more compact and cohesive film. This phenomenon is predominantly attributed to hydrogen bonding and van der Waals forces between the hydroxyl groups on the polymer chains of both agar and PG [34]. These molecular interactions facilitate closer packing of the polymer chains, thereby reducing the free volume within the matrix and leading to a denser, more structurally stable film [35]. Moreover, the compatible mixture of agar and PG within the polymer matrix may improve a semi-interpenetrating polymer network, where the polymers are partially linked while preserving their individual properties. This network structure further enhances the mechanical as well as the thermal stability of the film [36], as described later in the thermal behavior section (see Section 3.6).

However, an exception was observed in the A₅₀P₅₀ sample, whereas a decrease in EAB was noted. These results suggest that the balanced mixture (50:50) may lead to lower EAB. This phenomenon could be attributed to the weaker intermolecular chemical bonds between the two different biopolymers particularly at above the optimum blending ratio, in this case, is above a 25% PG inclusion to the agar matrix. In contrast, the intra-molecular chemical bonds in a single or predominantly one biopolymer are typically stronger. Therefore, when the polymers are mixed in equal proportions, the produced film may not achieve the same mechanical strength as films composed of a single polymer. This results is also in accordance with the finding reported by Ganesan et al. [33], that the excessive addition of konjac-glucomannan to polymeric seaweed's polysaccharide film may reduce intermolecular bonding interactions and elevate electrostatic repulsion between the two different biopolymers. However, this reduction in gel strength is compensated by an increase in the stretchability of the resulting film.

The overall findings suggested that the mechanical properties of the films are primarily determined by the inherent characteristics of each biopolymer used. Agar, which is known for its rigidity, contributes to the film's stiffness and inflexibility. In contrast, PG, which has a flexible nature, makes the film more stretchable and elastic. The combination of these two biopolymers creates a material with mechanical properties that reflect both agar's rigidity and PG's flexibility. Therefore, the overall mechanical behavior of the films results from the interplay between these contrasting biopolymer properties. To achieve a rigid texture, an increased quantity of agar is required. Conversely, a more elastic or stretchable texture can be obtained by using a higher proportion of PG. A similar finding was reported by Zou et al. [37] for composite films made from corn starch and konjac glucomannan, where increasing the glucomannan content in the film formulation enhanced the stretchability of the resulting films.

3.3 Water Vapor Permeability

As changes in food moisture content considerably affect its quality, it is necessary to prevent water vapor migration from the food to the environment or vice versa. The water vapor permeability (WVP) values, as shown in Fig. 1 illustrating the rate of moisture migration through the packaging film samples. From the graphs, there is a slight decrease in WVP after the inclusion of PG up to 50% with the lowest transfer rate of $2.40 \times 10^{-6} \text{ g}\cdot\text{mm}\cdot\text{cm}^{-2}\cdot\text{day}^{-1}\cdot\text{Pa}^{-1}$, but then followed by an increase with the further addition of higher PG concentrations. This phenomenon in accordance with the findings on the tensile strength of the film samples (see Table 2). The addition of a specific amount of PG into the agar-polymeric film resulted in optimum film compactness, whereas an excess of PG led to a reduction in the compactness of the polymer structure. A typical trend in WVP values was observed in composite films composed of starch and konjac glucomannan [37] whereas the addition of glucomannan to a certain threshold effectively reduced the WVP values of the films. However, exceeding this threshold resulted in an increase in WVP values.

These results are also supported by investigations reported by Qiao et al. [9] and Liu et al. [27], reported that the combination of agar and konjac glucomannan (extracted from *Amorphophallus konjac*) up to a certain proportion synergistically produces a more compact polymer structure. In such cases, a more compact film exhibits more effectiveness in impeding the migration of water vapor. In addition, the improvement in these barrier properties with the addition of PG up to 50% (A₅₀P₅₀) may also be attributed to increased film crystallinity [9], thereby increasing tortuosity within the polymer matrix against water vapor penetration [25,38].

Overall, the WVP values of the agar/PG films, ranging from 2.40 to $2.58 \times 10^{-6} \text{ g}\cdot\text{mm}\cdot\text{cm}^{-2}\cdot\text{day}^{-1}\cdot\text{Pa}^{-1}$, are comparable to those derived from starches, seaweed polysaccharides, also from gelatin [39,40]. However, when compared to bioplastic polyester films such as PLA and PHA, these values are considerably higher. PLA and PHA films typically exhibit WVP values in the range of 0.5×10^{-6} to $1.5 \times 10^{-6} \text{ g}\cdot\text{mm}\cdot\text{cm}^{-2}\cdot\text{day}^{-1}\cdot\text{Pa}^{-1}$ and 1.0×10^{-6} to $3.0 \times 10^{-6} \text{ g}\cdot\text{mm}\cdot\text{cm}^{-2}\cdot\text{day}^{-1}\cdot\text{Pa}^{-1}$, respectively [41,42].

Additionally, synthetic plastics like Low-Density Polyethylene (LDPE) and Polyethylene Terephthalate (PET) have even lower WVP values, around 0.01×10^{-6} to 0.1×10^{-6} $\text{g}\cdot\text{mm}\cdot\text{cm}^{-2}\cdot\text{day}^{-1}\cdot\text{Pa}^{-1}$ [42], demonstrating their superior moisture barrier properties, which make them more effective in protecting packaged food products [43]. Nonetheless, these findings suggest that agar/PG films are more suitable for applications where biodegradability is prioritized over moisture resistance.

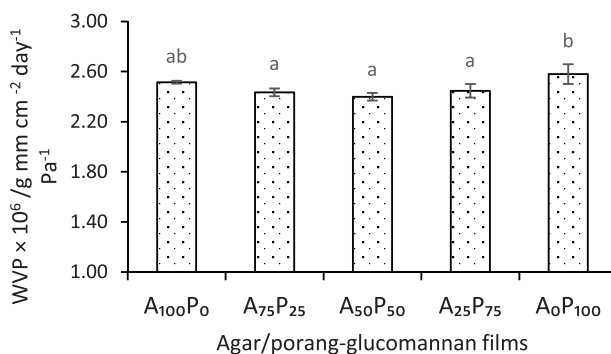


Figure 1: Water vapor permeability of agar/PG bioplastic films: A₁₀₀P₀ = 100:0, A₇₅P₂₅ = 75:25, A₅₀P₅₀ = 50:50, A₂₅P₇₅ = 25:75, and A₀P₁₀₀ = 0:100 of the agar and PG ratios (% w/w). Values are given as means with STDs. Any two means in the same column followed by the same letter are not significantly different ($p > 0.05$)

3.4 Scanning Electron Microscopy (SEM)

The microstructural appearance of the film surface is presented in Fig. 2. The cross-sectional images exhibited an overall homogeneous blend of both biopolymer agar and PG with no remarkable aggregation across the polymer matrix (see Fig. 2). A pure agar film (A₁₀₀P₀) exhibits a homogeneous surface structure and appears solid with no aggregation or disruptions across the matrix. However, subtle regular horizontal lines are identified across nearly the entire surface of the matrix, indicating the rigid nature of the pure agar film. When 25% PG is added to the agar polymeric film (A₇₅P₂₅), the matrix becomes more compact, as evidenced by the disappearance of the regular horizontal lines that were present in the pure agar film (A₁₀₀P₀). This change suggests that the two biopolymers are highly compatible, which in turn leads to greater structural integrity of the film matrix and may be associated with improved tensile properties.

However, when agar and PG are combined in equal proportions (A₅₀P₅₀), the structural integrity of the film matrix begins to decline. This decline is noticeable through the emergence of irregular lines and a rougher surface. Consequently, these changes are associated with a decrease in matrix compactness, which further leads to a reduction in mechanical properties such as flexibility and tensile strength (see Table 2). As the proportion of PG in the film matrix becomes more dominant (A₂₅P₇₅), similar to what was observed in agar-predominated film, an increase in film compactness is observed, along with a corresponding decrease in irregular lines and disruptions within the film structure. Finally, in the pure PG film (A₀P₁₀₀), again the structure appears less compact, with an increasing number of disruptions and several aggregations, possibly due to the presence of impurities particles originating from PG. The findings from this microstructural analysis provide a clear explanation for the measured mechanical properties and WVP values of the film samples, demonstrating a strong correlation between these characteristics and the structural integrity of the film matrix.

3.5 Fourier Transform Infrared Spectroscopy

The spectra presented in Fig. 3 demonstrate a similarity in the chemical structures of the two polysaccharides. This was evident when comparing films produced from pure agar (A₁₀₀P₀) and pure PG

(A₀P₁₀₀). Notably, distinct absorption bands of those two biopolymers are only observable in spectra with wavelengths of less than 1000 cm⁻¹. The spectral analysis showed that the film made entirely of 100% agar (A₁₀₀P₀) exhibits a broad absorption band around 3286 cm⁻¹, which is attributed to the stretching vibrations of -OH groups. Additionally, the peaks appear around 2931 cm⁻¹ represent the stretching of C-H groups associated with methine rings in the agar hydrogen bond. The peak at approximately 1639 cm⁻¹ suggests the stretching of conjugated peptide bonds formed by amine (-NH) and acetone (-CO) groups. Furthermore, the peak at 1369 cm⁻¹ is associated with sulfate groups, and peaks at 1068, 1037, and 930 cm⁻¹ ascribe to the stretching vibrations of C-O 3,6 anhydro-galactose [44].

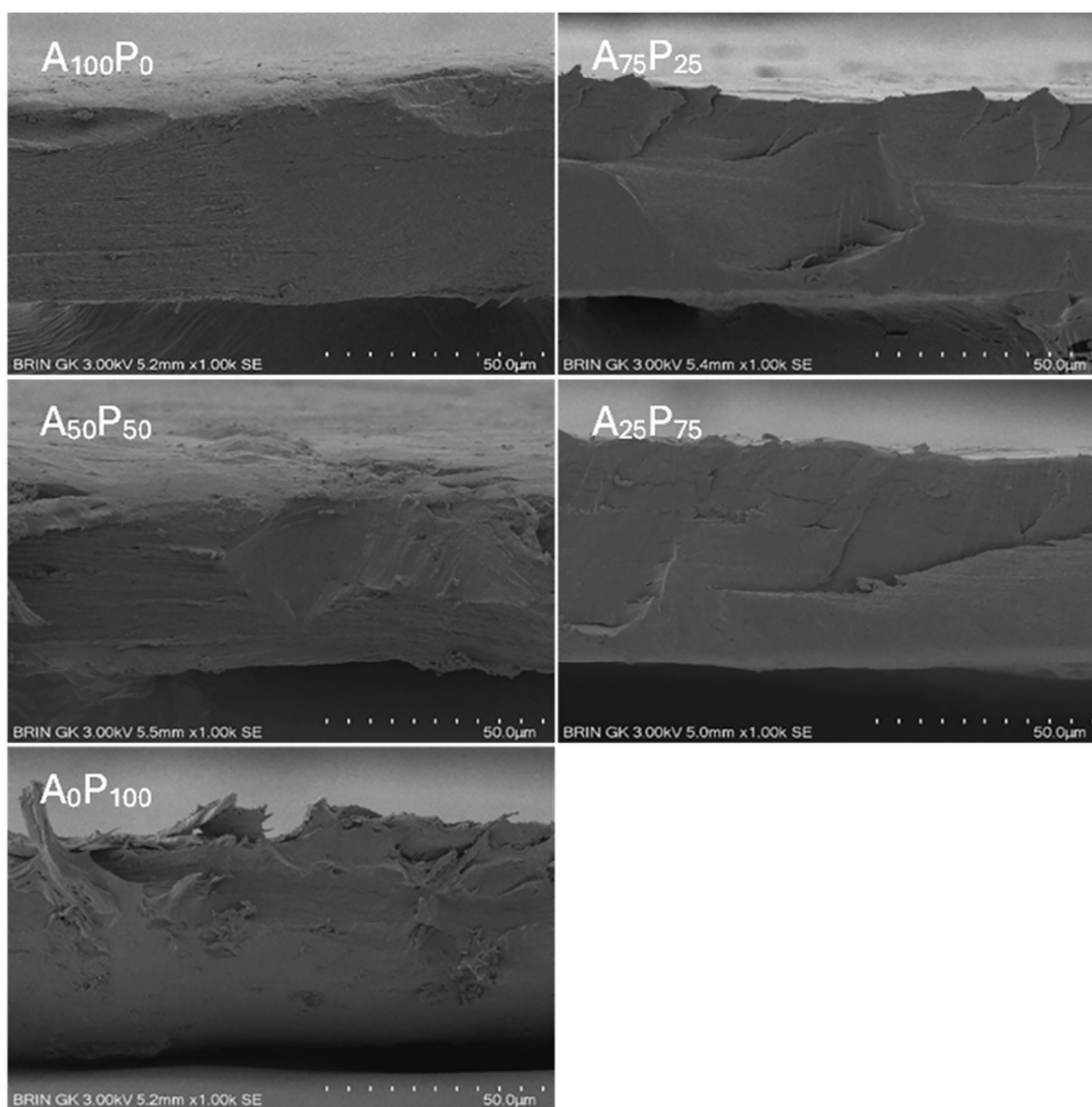


Figure 2: Cross-sectional surface images of agar/PG bioplastic films: A₁₀₀P₀ = 100:0, A₇₅P₂₅ = 75:25, A₅₀P₅₀ = 50:50, A₂₅P₇₅ = 25:75, and A₀P₁₀₀ = 0:100 of the agar and PG ratios (% w/w)

The film composed entirely of PG (A₀P₁₀₀) demonstrated absorption bands remarkably similar to those observed in konjac glucomannan [45]. Specifically, there was a peak around 3297 cm⁻¹ corresponding to the stretching vibrations of -OH groups, while the peak at 2881 cm⁻¹ was associated to the stretching vibrations

of methyl C-H groups in PG. Additionally, the peak at 1724 cm^{-1} was likely due to the stretching vibrations of acetyl groups [24], and the peak at 1643 cm^{-1} indicated C-O stretching associated with the presence of water [46]. Furthermore, peaks at 871 and 806 cm^{-1} were identified and associated with mannose stretching in PG [47,48].

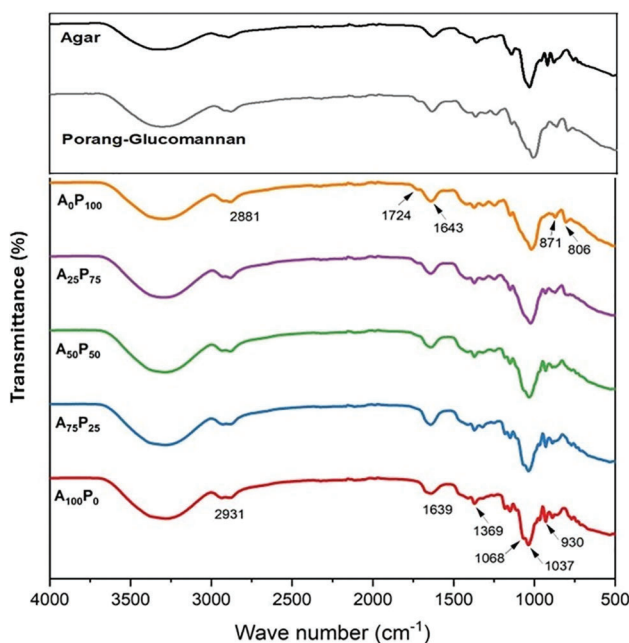


Figure 3: FTIR (Fourier Transform Infrared Spectroscopy) of agar, porang-glucomannan, and the bioplastic films: $A_{100}P_0 = 100:0$, $A_{75}P_{25} = 75:25$, $A_{50}P_{50} = 50:50$, $A_{25}P_{75} = 25:75$, and $A_0P_{100} = 0:100$ of the agar and PG ratios (% w/w)

The absorption peak at 1068 cm^{-1} corresponds to the molecular crystallization area in a polysaccharide film, while the peak at 1037 cm^{-1} reflects its amorphous structure [49]. The absorbance ratio of 1068 cm^{-1} to 1037 cm^{-1} is associated with the degree of molecular chain order in the film. The spectra suggest that increasing the proportion of PG in the polymer matrix reduces the ratio of crystallized to amorphous regions. This reduction indicates a decrease in short-range order within the polymeric film structure, which is followed by the formation of additional linkages among agar molecules due to the excess PG content. However, the films containing a blend of agar and PG overall exhibited positional absorption bands that were consistent across all formulations, with no new peaks observed. This suggests that the combination of agar and PG did not induce significant changes in their chemical structures. Furthermore, these results might indicate that both polysaccharides are compatible, which results in a homogeneous blend, as corroborated by the microstructural images previously presented (see Fig. 2).

3.6 Thermal Stability

An interesting finding from the thermal analysis of both polymeric agar and PG films is their nearly identical thermal decomposition behavior, suggesting that both biopolymers exhibit comparable thermal stability. However, a more detailed evaluation, specifically through the analysis of dTG thermograms of the samples with the most distinct formulations, i.e., pure agar film and pure PG film (see Fig. 4a), exhibits that each biopolymer undergoes three stages of thermal decomposition (see Fig. 4b).

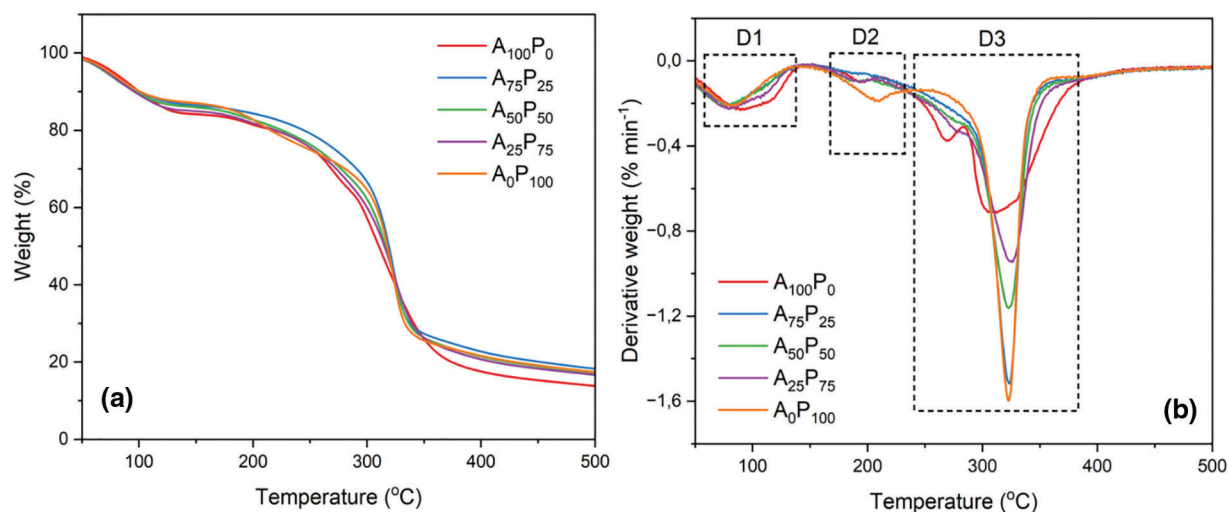


Figure 4: TG (a) and dTG (b) analysis of agar/PG bioplastic films: $A_{100}P_0 = 100:0$, $A_{75}P_{25} = 75:25$, $A_{50}P_{50} = 50:50$, $A_{25}P_{75} = 25:75$, and $A_0P_{100} = 0:100$ of the agar and PG ratios (% w/w)

The first stage of thermal decomposition (D1) occurred in the temperature range between 70°C – 120°C , marked by the loss of sample weight due to the evaporation of water and certain volatile compounds with low molecular weight from the film matrix structure. Subsequently, a distinct thermal behavior was observed during the second stage of decomposition (D2) between the agar- and PG-dominated films. The agar-dominated film began decomposing earlier at approximately 190°C with a lower decomposition intensity, while the PG-dominated film decomposed at a higher temperature, around 205°C . This second decomposition is likely due to the degradation of the plasticizer glycerol [50,51]. Furthermore, in the major decomposition stage (D3), the agar-dominated films exhibited two distinct decomposition peaks at about 265°C and 310°C , whereas the PG-dominated films showed only one peak at approximately 320°C . The initial peak observed in the agar-dominated film likely corresponds to the degradation of agar's primary chemical structure, coinciding with the degradation of the remaining glycerol plasticizer. As the temperature increased to the range of 310°C – 320°C , both films experienced degradation of their primary polymeric components, involving the cleavage of hydrogen bonds and the decomposition of the saccharide rings in both agar and glucomannan [52]. Additionally, some residual organic components present in agar and PG, such as cellulose, also underwent decomposition during this stage [53].

Based on these findings, it can be assumed that the film samples with higher PG content demonstrated greater thermal stability compared to the films with higher agar content, notably observed during the second and third/major decomposition. Moreover, the observed residues at temperatures exceeding 350°C suggested that films with higher PG content exhibit greater residual weights. This phenomenon might be attributed to the presence of impurity compounds in PG, particularly cellulose. An increase in thermal stability was also reported by Gomes Neto et al. [54] for chitosan films blended with glucomannan.

The DSC thermogram showed that the endothermic peaks of both pure agar and pure PG films shifted to lower temperatures after they were combined (see Fig. 5). These endothermic peaks not only indicate the evaporation of water molecules from the polymeric films but may also correspond to the softening of the polymer matrix or the glass transition process (T_g). This shifting suggests a decrease in the thermal stability of the films, especially in those with an equal proportion ($A_{50}P_{50}$). The decrease in thermal stability could be attributed to the interaction between the two polymers, which might disrupt the crystalline regions within the polymer matrix, leading to a less thermally stable structure. This

phenomenon is further linked to the compactness of the polymer film structure, which also explains the observed variations in tensile strength (see Table 2) and water vapor permeability (see Fig. 1).

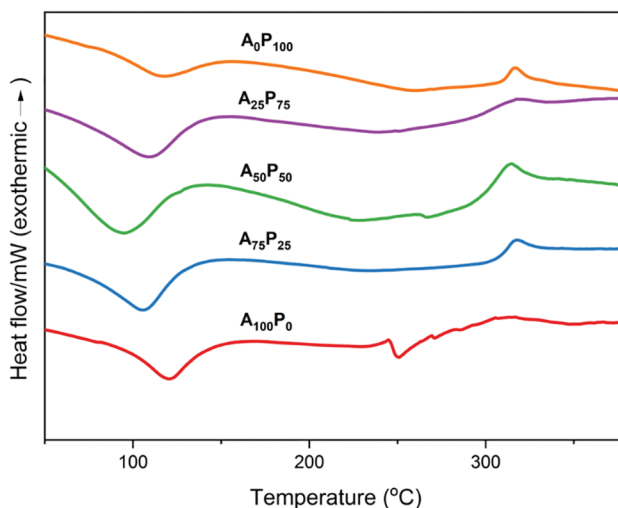


Figure 5: DSC thermograms of agar/PG bioplastic films: $A_{100}P_0 = 100:0$, $A_{75}P_{25} = 75:25$, $A_{50}P_{50} = 50:50$, $A_{25}P_{75} = 25:75$, and $A_0P_{100} = 0:100$ of the agar and PG ratios (% w/w)

Furthermore, a distinct second endothermic peak was identified around 250°C in samples with a higher agar composition. This more pronounced peak indicates a melting (T_m) process in the agar biopolymeric film, which was not observed in the PG film samples. Finally, there was an observed shift in the exothermic peak towards higher temperatures as the amount of PG in the film matrix increased, particularly in the temperature range of 310°C – 320°C . These peaks were associated with the thermal decomposition of the molecular structure of the film samples. These findings support the previously explained phenomenon of the third-stage thermal decomposition observed in TG and DTG analyses. In this context, the sample films with higher PG content exhibit increased resistance to degradation at temperatures above 300°C , attributed to their impurities content.

4 Conclusion

The utilization of porang-glucomannan (*Amorphophallus oncophyllus*) in this study has successfully improved the characteristics of agar-based films, particularly by enhancing the flexibility of the resulting film, which is essential for its application as a food packaging material. However, the enhancement in mechanical properties is offset by a decrease in water sensitivity in the resulting films. The observations specifically demonstrated that incorporating PG into the polymeric agar at an optimal threshold of 25% (w/w) in the total formulation enhanced the compactness of the polymer film structure. This resulted in an increase of over 100% in elongation at break, a 37.4% increase in tensile strength, and a 3.2% reduction in moisture barrier. Additionally, the thermal stability of the resulting film was also increased. However, exceeding this threshold overall led to a decrease in the intermolecular structure of the polymer film, which subsequently diminished its overall properties. Based on the observations, it can be concluded that the characteristics of the films derived from the agar and PG biopolymers reflect a resultant of the inherent properties of each material. These findings also suggest the potential of combining agar and PG as raw materials for food packaging due to their adaptable properties through the adjustment of their composition.

Acknowledgement: The authors extend their gratitude to the Faculty of Agricultural Technology, Gadjah Mada University for their significant contributions, specifically through providing porang-glucomannan (PG) and access to laboratory equipment.

Funding Statement: This work was funded by a research grant from the Lembaga Pengelola Dana Pendidikan—Ministry of Finance Republic of Indonesia (<https://risprolpdp.kemenkeu.go.id/>) (accessed on 13 September 2024), awarded under the Riset dan Inovasi untuk Indonesia Maju program with grant number 82/II.7/HK/2022.

Author Contributions: The authors confirm their contribution to the paper as follows: **Toni Dwi Novianto:** Study conception and design, data collection, draft manuscript preparation, analysis and interpretation of results. **Bakti Berlyanto Sedayu:** Study conception and design, writing—review & editing, analysis and interpretation of results, visualization, supervision. **Sri Rahayoe:** Study conception and design, writing—review & editing, analysis and interpretation of results, supervision. All authors reviewed the results and approved the final version of the manuscript.

Availability of Data and Materials: All data generated and analyzed during this study are included in this article.

Ethics Approval: This work did not include any human subjects or animal experiments.

Conflicts of Interest: The authors declare no conflicts of interest to report regarding the present study.

References

1. González-López ME, Calva-Estrada SdJ, Gradilla-Hernández MS, Barajas-Álvarez P. Current trends in biopolymers for food packaging: a review. *Front Sustainable Food Syst.* 2023;7:1–20. doi:10.3389/fsufs.2023.1225371.
2. Kibria MG, Masuk NI, Safayet R, Nguyen HQ, Mourshed M. Plastic waste: challenges and opportunities to mitigate pollution and effective management. *Int J Environ Res.* 2023;17(1):20. doi:10.1007/s41742-023-00507-z.
3. Macht J, Klink-Lehmann J, Venghaus S. Eco-friendly alternatives to food packed in plastics: German consumers' purchase intentions for different bio-based packaging strategies. *Food Qual Prefer.* 2023;109:104884. doi:10.1016/j.foodqual.2023.104884.
4. Asgher M, Qamar SA, Bilal M, Iqbal HMN. Bio-based active food packaging materials: sustainable alternative to conventional petrochemical-based packaging materials. *Food Res Int.* 2020;137:109625. doi:10.1016/j.foodres.2020.109625.
5. Sedayu BB, Cran MJ, Bigger SW. A review of property enhancement techniques for carrageenan-based films and coatings. *Carbohydr Polym.* 2019;216:287–302. doi:10.1016/j.carbpol.2019.04.021.
6. George N, Venugopal B. Gas barrier properties of biopolymers. In: Thomas S, Ar A, Jose Chirayil C, Thomas B, editors. *Handbook of biopolymers.* Singapore: Springer Nature Singapore; 2023. p. 297–321.
7. Martínez-Sanz M, Martínez-Abad A, López-Rubio A. Cost-efficient bio-based food packaging films from unpurified agar-based extracts. *Food Packag Shelf Life.* 2019;21:100367. doi:10.1016/j.fpsl.2019.100367.
8. Iribarren E, Wongphan P, Bumbudsanpharoke N, Chonhenchob V, Jarupan L, Harnkarnsujarit N. Thermoplastic agar blended PBAT films with enhanced oxygen scavenging activity. *Food Biosci.* 2023;54:102940. doi:10.1016/j.fbio.2023.102940.
9. Qiao D, Tu W, Zhong L, Wang Z, Zhang B, Jiang F. Microstructure and mechanical/hydrophilic features of agar-based films incorporated with konjac glucomannan. *Polymers.* 2019;11(12):1952. doi:10.3390/polym11121952.
10. Mostafavi FS, Zaeim D. Agar-based edible films for food packaging applications—a review. *Int J Biol Macromol.* 2020;159:1165–76. doi:10.1016/j.ijbiomac.2020.05.123.

11. Huang Q, Jin W, Ye S, Hu Y, Wang Y, Xu W, et al. Comparative studies of konjac flours extracted from *Amorphophallus guripingensis* and *Amorphophallus rivirei*: based on chemical analysis and rheology. *Food Hydrocoll.* 2016;57:209–16. doi:10.1016/j.foodhyd.2016.01.017.
12. Shi X-D, Yin J-Y, Zhang L-J, Huang X-J, Nie S-P. Studies on *O*-acetyl-glucomannans from *Amorphophallus* species: comparison of physicochemical properties and primary structures. *Food Hydrocoll.* 2019;89:503–11. doi:10.1016/j.foodhyd.2018.11.013.
13. Yanuriati A, Marseno DW, Harmayani E. Characteristics of glucomannan isolated from fresh tuber of Porang (*Amorphophallus muelleri* Blume). *Carbohydr Polym.* 2017;156:56–63. doi:10.1016/j.carbpol.2016.08.080.
14. Warkoyo PI, Siskawardani DD, Husna A. The effect of konjac glucomannan and Aloe vera gel concentration on physical and mechanical properties of edible film. *Food Res.* 2022;6(3):298–305. doi:10.26656/fr.2017.
15. Harmayani E, Aprilia V, Marsono Y. Characterization of glucomannan from *Amorphophallus oncophyllus* and its prebiotic activity *in vivo*. *Carbohydr Polym.* 2014;112:475–9. doi:10.1016/j.carbpol.2014.06.019.
16. Mitri A, Maghfirah A, Brahmana K, Sudiati. Effect of gelatinization temperature on the physical properties of Porang (*Amorphophallus oncophyllus*) starch bioplastics with sorbitol plasticizer. *J Technomat Phys.* 2023;5(1):33–8. doi:10.32734/jotpv5i1.10217.
17. Maghfirah A, Sudiati, Sitepu SNKB, Siambaton MW. The effect of using a combination of sorbitol and glycerol plasticizers on the characterization of edible film from Porang (*Amorphophallus oncophyllus*) starch. *J Technomat Phys.* 2023;5(2):86–92. doi:10.32734/jotpv5i2.12397.
18. Qiao D, Wang Z, Cai C, Yin S, Qian H, Zhang B, et al. Tailoring multi-level structural and practical features of gelatin films by varying konjac glucomannan content and drying temperature. *Polymers.* 2020;12(2):385. doi:10.3390/polym12020385.
19. Anissa MN, Rahayoe S, Harmayani E, Ulya KN. Extraction and characterization of glucomannan from Porang (*Amorphophallus oncophyllus*) with size variations of Porang. *Agritech.* 2023;43(4):328–34. doi:10.22146/agritech.68886.
20. Peng S, Zhang J, Zhang T, Hati S, Mo H, Xu D, et al. Characterization of carvacrol incorporated antimicrobial film based on agar/konjac glucomannan and its application in chicken preservation. *J Food Eng.* 2022;330:111091. doi:10.1016/j.jfoodeng.2022.111091.
21. Valizadeh S, Naseri M, Babaei S, Hosseini SMH, Imani A. Development of bioactive composite films from chitosan and carboxymethyl cellulose using glutaraldehyde, cinnamon essential oil and oleic acid. *Int J Biol Macromol.* 2019;134:604–12. doi:10.1016/j.ijbiomac.2019.05.071.
22. Xiao M, Luo L, Tang B, Qin J, Wu K, Jiang F. Physical, structural, and water barrier properties of emulsified blend film based on konjac glucomannan/agar/gum Arabic incorporating virgin coconut oil. *LWT.* 2022;154:112683. doi:10.1016/j.lwt.2021.112683.
23. Sedayu BB, Cran MJ, Bigger SW. Effects of surface photocrosslinking on the properties of semi-refined carrageenan film. *Food Hydrocoll.* 2021;111:106196. doi:10.1016/j.foodhyd.2020.106196.
24. Qiao D, Lu J, Chen Z, Liu X, Li M, Zhan B. Zein inclusion changes the rheological, hydrophobic and mechanical properties of agar/konjac glucomannan based system. *Food Hydrocoll.* 2023;137:108365. doi:10.1016/j.foodhyd.2022.108365.
25. Sedayu BB, Cran MJ, Bigger SW. Reinforcement of refined and semi-refined carrageenan film with nanocellulose. *Polymers.* 2020;12(5):1145. doi:10.3390/polym12051145.
26. Da Rocha M, Alemán A, Romani VP, López-Caballero ME, Gómez-Guillén MC, Montero P, et al. Effects of agar films incorporated with fish protein hydrolysate or clove essential oil on flounder (*Paralichthys orbignyanus*) fillets shelf-life. *Food Hydrocoll.* 2018;81:351–63. doi:10.1016/j.foodhyd.2018.03.017.
27. Liu Z, Lin D, Lopez-Sanchez P, Yang X. Characterizations of bacterial cellulose nanofibers reinforced edible films based on konjac glucomannan. *Int J Biol Macromol.* 2020;145:634–45. doi:10.1016/j.ijbiomac.2019.12.109.
28. Sun Y, Xu X, Zhang Q, Zhang D, Xie X, Zhou H, et al. Review of konjac glucomannan structure, properties, gelation mechanism, and application in medical biology. *Polymers.* 2023;15(8):1852. doi:10.3390/polym15081852.

29. Choi I, Hong W, Lee J-S, Han J. Influence of acetylation and chemical interaction on edible film properties and different processing methods for food application. *Food Chem.* 2023;426:136555. doi:10.1016/j.foodchem.2023.136555.
30. Yadav M, Chiu F-C. Cellulose nanocrystals reinforced κ -carrageenan based UV resistant transparent bionanocomposite films for sustainable packaging applications. *Carbohydr Polym.* 2019;211:181–94. doi:10.1016/j.carbpol.2019.01.114.
31. Kumar A, Srivastav PP, Pravitha M, Hasan M, Mangaraj S, Prithviraj V, et al. Comparative study on the optimization and characterization of soybean aqueous extract based composite film using response surface methodology (RSM) and artificial neural network (ANN). *Food Packag Shelf Life.* 2022;31:100778. doi:10.1016/j.fpsl.2021.100778.
32. Yanuriati A, Basir D. Peningkatan kelarutan glukomanan porang (*Amorphophallus muelleri* Blume) dengan penggilangan basah dan kering. *Agritech.* 2020;40(3):223–31 (in Indonesian). doi:10.22146/agritech.43684.
33. Ganesan AR, Shanmugam M, Ilansuriyan P, Anandhakumar R, Balasubramanian B. Composite film for edible oil packaging from carrageenan derivative and konjac glucomannan: application and quality evaluation. *Polym Test.* 2019;78:105936. doi:10.1016/j.polymertesting.2019.105936.
34. Iheanacho BC, Ajoge HN, Ismail U, Zoum FA, Ifeanyi-Nze FO, Okunbi FO, et al. A comprehensive study on the production and characterization of eco-friendly biodegradable plastic films from dent corn starch. *Arch Adv Eng Sci.* 2024;1–10. doi:10.47852/bonviewAAES42022946.
35. Dutta D, Sit N. Comprehensive review on developments in starch-based films along with active ingredients for sustainable food packaging. *Sustain Chem Pharm.* 2024;39:101534. doi:10.1016/j.scp.2024.101534.
36. Pei J, Palanisamy CP, Srinivasan GP, Panagal M, Kumar SSD, Mironescu M. A comprehensive review on starch-based sustainable edible films loaded with bioactive components for food packaging. *Int J Biol Macromol.* 2024;274:133332. doi:10.1016/j.ijbiomac.2024.133332.
37. Zou Y, Yuan C, Cui B, Liu P, Wu Z, Zhao H. Formation of high amylose corn starch/konjac glucomannan composite film with improved mechanical and barrier properties. *Carbohydr Polym.* 2021;251:117039. doi:10.1016/j.carbpol.2020.117039.
38. Shahbazi M, Ahmadi SJ, Seif A, Rajabzadeh G. Carboxymethyl cellulose film modification through surface photocrosslinking and chemical crosslinking for food packaging applications. *Food Hydrocoll.* 2016;61:378–89. doi:10.1016/j.foodhyd.2016.04.021.
39. Shanbhag C, Shenoy R, Shetty P, Srinivasulu M, Nayak R. Formulation and characterization of starch-based novel biodegradable edible films for food packaging. *J Food Sci Technol.* 2023;60(11):2858–67. doi:10.1007/s13197-023-05803-2.
40. Charles AL, Motsa N, Abdillah AA. A comprehensive characterization of biodegradable edible films based on potato peel starch plasticized with glycerol. *Polymers.* 2022;14(17):3462. doi:10.3390/polym14173462.
41. Apicella A, Barbato A, Garofalo E, Incarnato L, Scarfato P. Effect of PVOH/PLA + wax coatings on physical and functional properties of biodegradable food packaging films. *Polymers.* 2022;14(5):935. doi:10.3390/polym14050935.
42. Wang LZ, Liu L, Holmes J, Kerry JF, Kerry JP. Assessment of film-forming potential and properties of protein and polysaccharide-based biopolymer films. *Int J Food Sci Technol.* 2007;42(9):1128–38. doi:10.1111/j.1365-2621.2006.01440.x.
43. Chakraborty INP, Banik S, Govindaraju I, Das K, Mal SS, Zhuo GY, et al. Synthesis and detailed characterization of sustainable starch-based bioplastic. *J Appl Polym Sci.* 2022;139(39):e52924. doi:10.1002/app.52924.
44. Zhang R, Wang W, Zhang H, Dai Y, Dong H, Hou H. Effects of hydrophobic agents on the physicochemical properties of edible agar/maltodextrin films. *Food Hydrocoll.* 2019;88:283–90. doi:10.1016/j.foodhyd.2018.10.008.
45. Ouyang D, Deng J, Zhou K, Liang Y, Chen Y, Wang D, et al. The effect of deacetylation degree of konjac glucomannan on microbial metabolites and gut microbiota *in vitro* fermentation. *J Funct Foods.* 2020;66:103796. doi:10.1016/j.jff.2020.103796.
46. Wu C, Peng S, Wen C, Wang X, Fan L, Deng R, et al. Structural characterization and properties of konjac glucomannan/curdlan blend films. *Carbohydr Polym.* 2012;89(2):497–503. doi:10.1016/j.carbpol.2012.03.034.

47. Ye X, Kennedy J, Li B, Xie B. Condensed state structure and biocompatibility of the konjac glucomannan/chitosan blend films. *Carbohydr Polym.* 2006;64(4):532–8. doi:10.1016/j.carbpol.2005.11.005.
48. Li X, Jiang F, Ni X, Yan W, Fang Y, Corke H, et al. Preparation and characterization of konjac glucomannan and ethyl cellulose blend films. *Food Hydrocoll.* 2015;44:229–36. doi:10.1016/j.foodhyd.2014.09.027.
49. Man J, Yang Y, Zhang C, Zhou X, Dong Y, Zhang F, et al. Structural changes of high-amylose rice starch residues following *in vitro* and *in vivo* digestion. *J Agric Food Chem.* 2012;60(36):9332–41. doi:10.1021/jf302966f.
50. Reddy JP, Rhim J-W. Characterization of bionanocomposite films prepared with agar and paper-mulberry pulp nanocellulose. *Carbohydr Polym.* 2014;110:480–8. doi:10.1016/j.carbpol.2014.04.056.
51. Mohajer S, Rezaei M, Hosseini SF. Physico-chemical and microstructural properties of fish gelatin/agar bio-based blend films. *Carbohydr Polym.* 2017;157:784–93. doi:10.1016/j.carbpol.2016.10.061.
52. Zou Y, Yuan C, Cui B, Sha H, Liu P, Lu L, et al. High-amylose corn starch/konjac glucomannan composite film: reinforced by incorporating β -cyclodextrin. *J Agric Food Chem.* 2021;69(8):2493–500. doi:10.1021/acs.jafc.0c06648.
53. Moriana R, Zhang Y, Mischnick P, Li J, Ek M. Thermal degradation behavior and kinetic analysis of spruce glucomannan and its methylated derivatives. *Carbohydr Polym.* 2014;106:60–70. doi:10.1016/j.carbpol.2014.01.086.
54. Gomes Neto RJ, Genevro GM, Paulo LDA, Lopes PS, de Moraes MA, Beppu MM. Characterization and *in vitro* evaluation of chitosan/konjac glucomannan bilayer film as a wound dressing. *Carbohydr Polym.* 2019;212:59–66. doi:10.1016/j.carbpol.2019.02.017.